



Effect of pad eye position on anchor pile response and soil displacement field under oblique pullout load

Zhongtao Wang*

Dalian University of Technology, Dalian, P.R. China

Guangyu Luo

Dalian University of Technology, Dalian, P.R. China

*zhongtao@dlut.edu.cn

ABSTRACT: Anchor piles have been extensively utilized to support offshore floating platform and must have sufficient bearing capacity to resist oblique pullout loads transmitted from mooring chains. The bearing capacity of anchor piles under oblique pullout loads depends on pad eye positions (z/L , L is the pile length). However, the effect of pad eye positions on the anchor pile response and soil displacement field is still unclear. Based on transparent sand, a series of centrifuge model tests were performed on the anchor pile subjected to oblique pullout loads. The pile capacity and soil displacement under different pad eye positions were studied. It shows that with the increase of the pad eye position, the rotation direction of the anchor pile gradually changed from forward rotation to backward rotation, and the deformation range and displacement value (especially horizontal displacement) of deep soil increased. Therefore, the pile bearing capacity with $z/L = 0.55, 0.67$ and 0.75 improved 45%, 76% and 131% of that with $z/L = 0.40$. As the pad eye position increased from $0.67L$ to $0.75L$, the pile failure mode transformed from vertically dominated pulling to translation with rotation and lateral deflection, and the displacement value and ratio of horizontal to vertical displacement increased by 30% and 36% in deep soil, respectively.

Keywords: Anchor pile; Pad eye position; Transparent sand; Oblique pullout load; Centrifuge model test

1 INTRODUCTION

With the development of offshore oil and gas resources, floating platforms anchored by mooring chains and pile foundations have been widely used. Different from other types of pile foundations, anchor piles are subjected to oblique pullout loads transmitted from mooring chains. The response of the anchor piles in sand under oblique pullout loads has been studied based on centrifuge model tests (Ramadan et al., 2013; Huang et al., 2020; Santiago et al., 2020). Among these investigations, the loading points were arranged near the pile head. However, an embedded pad eye of anchor piles was always set to resist more environmental loads. A series of studies have been conducted to analyze the effect of pad eye position on suction anchor capacity (Aubeny et al., 2003; Bang et al., 2011; Gao et al., 2013; Zhao et al., 2019; Cheng et al., 2021), however, anchor piles have greater aspect ratio, and there may be different effects of pad eye position on anchor pile response.

The response of anchor piles under oblique pullout load depends on the interaction between pile and soil, however, it is difficult to accurately measure internal displacement field of soil around the pile by conventional technical methods. In recent years, the measurement of internal soil displacement field has

been effectively solved by the combination of transparent soil materials and Particle Image Velocimetry (PIV) technology. Transparent soils consist of aggregate materials and pore fluids with an identical refractive index to permit the complete penetration of visible light. However, the limited visual range of transparent soil restricts the testing chamber geometry, leading to the soil stress loss caused by small-scale models. Centrifuge model tests can solve the problem by applying centrifugal acceleration. Previous centrifuge model tests using transparent soil have been performed to obtain the plate anchor trajectory during the keying process (Song et al., 2009) and the soil displacement field during the strip foundation settlement (Black, 2015). However, the soil displacement field around anchor piles under oblique pullout load has not been reported.

In this paper, centrifuge model tests through transparent soil were conducted on the anchor pile under oblique pullout load. The effect of pad eye position on anchor pile response and soil displacement field was investigated. The experimental results aim to provide technical support for the pad eye design of anchor piles.

2 EXPERIMENTAL SETUP

2.1 Testing system

The centrifugal model tests were performed in the drum geo-centrifuge GT450/1.4 at Dalian University of Technology. The testing system consists of a testing chamber, a linear laser, an action camera, steel wire rope, a load cell and an actuator, as shown in Figure 1. The dimensions of the chamber were 238 mm (radial depth) \times 330 mm (vertical width) \times 424 mm (circumferential width). The outer wall of the chamber was made of aluminum, the inner panels and cover plate were made of transparent plexiglass. The middle of the bottom plate was equipped with a camera case, and the middle line of the side plate was equipped with a movable pulley to adjust the loading angle. The laser device (FU520AL1200-GD22) was fixed on the actuator connection plate. The laser wavelength was 520 nm, and the maximum power of the laser device was 1.2 W. The camera (HERO9 Black) was ruggedized by the case, with a resolution of 2704×2028 pixels and a capture frequency of 50 Hz during the test. The diameter of the wire rope was 1.0 mm, and the maximum bearing capacity of the wire rope can reach 637 N. The load cell (CSF-3A) with a capacity of 800 N was hinged to the connecting plate, which ensured the load cell axis was in line with the loading direction. The test data were collected and processed in real time using a wireless data acquisition system developed by the University of Western Australia.

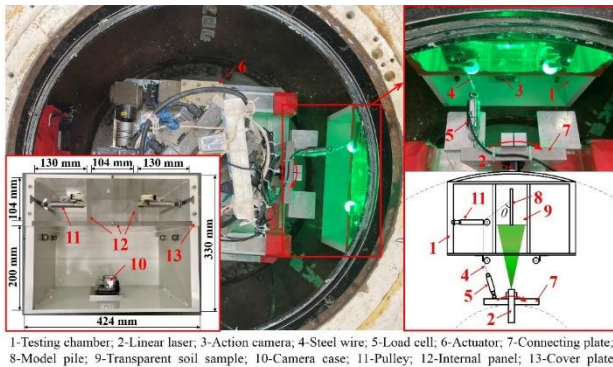


Figure 1. Centrifuge model test system on anchor pile based on transparent sand

2.2 Transparent soil material

The transparent soil used in this paper was made from fused quartz and pore fluid with an identical refractive index of 1.4585 at 24°C. The pore fluid was a blend of N-Paraffin Norpar 12 and White Oil 15 in the weight ratio of 1:4. The mechanical properties of this transparent soil are similar to natural sand (Ezzein and Bathurst, 2011; Guzman et al., 2014), and the transparent sand can form clear speckles under laser

illumination. To improve the visual range, the grain size of the fused quartz was 0.5~1.0 mm with a transparency of 15 cm and the curve of grain size distribution is shown in Figure 2. The minimum and maximum dry density equaled 0.970 g/cm^3 and 1.274 g/cm^3 , respectively. The internal friction angle of the transparent sand with 70% relative density was 39.4° (Kong et al., 2015).

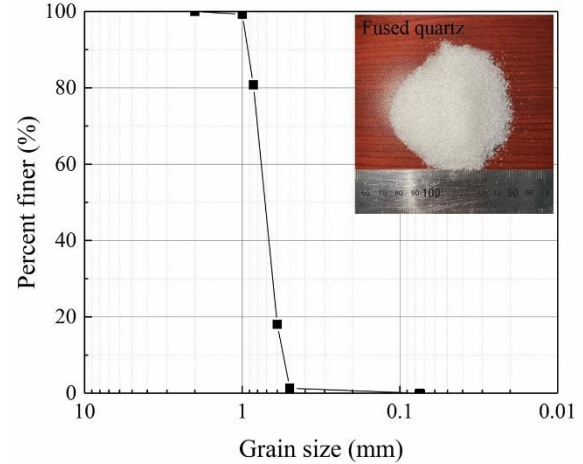


Figure 2. Grain size distribution for fused quartz

2.3 Anchor pile model

Open-ended pipe piles were fabricated from plexiglass to reduce the laser reflection. Anchor piles were selected as the anchoring foundation for a floating production storage offloading vessel at the Grand Banks of Newfoundland, Canada (Ramadan et al., 2013). The diameter (d) and length (L) of the anchor piles were 2 m and 30 m, respectively. According to the engineering background and testing chamber dimensions, the diameter and length of the model pile were 8 mm and 120 mm as large as possible, and the thickness was 1.5 mm. By referring the optimal pad eye position of suction anchors in sand, the pad eye position (z) was $0.40L$, $0.55L$, $0.67L$ and $0.75L$ away from the pile head, as shown in Figure 3.

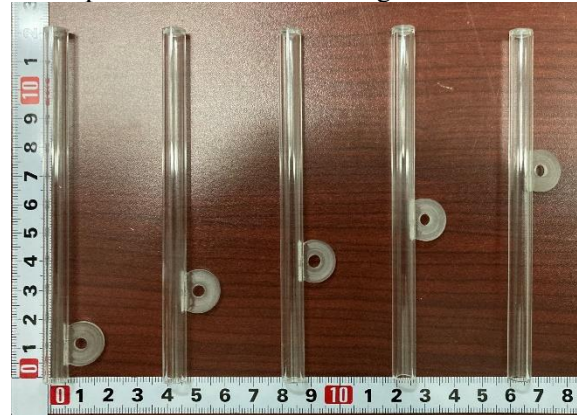


Figure 3. Anchor pile model with different pad eye positions

2.4 Model preparation and testing procedure

The procedure of centrifuge model tests were as follows. Firstly, the pile was suspended in the center of the empty chamber through a guide rod, and the pile end was 16 mm away from the chamber bottom to weaken the boundary effect (Georgiadis et al., 1992). The wire rope was connected to the model pile via the pad eye and taken over the pulley. Mooring chains make a vertical angle between 45° and 60° of the pad eye in deep water (Guo et al., 2018), therefore, an intermediate loading angle of 53° was selected by adjusting the pulley level. Secondly, the pore fluid was slowly poured into the chamber, and the fused quartz with the specified quality was poured into the pore fluid. The guide rod was removed when the fused quartz surface was near the pile head. The model chamber was put into the vacuum box to remove the air in the transparent sand sample. Thirdly, a plexiglass plate was placed on top of the transparent sand, and vertical static pressure was applied on the plate to flush the fused quartz surface with the pile head. The transparent sand sample can achieve a target relative density of about 70% by controlling the fused quartz quality and the transparent sand volume. Fourthly, the model chamber was mounted in the drum channel, and the other end of the steel wire was connected to the load cell. Fifthly, the centrifugal acceleration was raised to reach 50g, and the wire rope was pulled through the relative rotation between the actuator and the drum channel to apply a load to the pile. The relative rotation speed was set at $2.25^\circ/100\text{ s}$ to ensure drained conditions (Dyson and Randolph, 2001). The conditions of the centrifuge model test are summarized in Table 1.

Table 1. Summary of centrifuge model tests

L/d	Loading position (z/L)	Loading angle ($^\circ$)	Pullout bearing capacity (kN)
15	0.40	53	127.33
	0.55	53	184.72
	0.67	53	223.92
	0.75	53	294.14

3 RESULTS AND DISCUSSION

3.1 Load-displacement curves

The variation of pullout load with total displacement of pad eye under different pad eye positions is shown in Figure 4. It is noted that all the test results were presented at prototype scale. It was apparent that the load-displacement curves had nonlinear characteristics and could be roughly divided into three stages, namely the initial stage, the transition stage and the final stage. In the initial stage, the load on the anchor pile

increased rapidly with the increase of pad eye displacement. In the transition stage, the load continued increasing with the displacement, but the increasing velocity of the load gradually decreased. In the final stage, when the pad eye position was no more than $0.67L$, the load almost no longer changed with the increasing displacement because the pile was pulled out, and the load-displacement curves had a stable stage. However, when the pad eye position was $0.75L$, the load kept increasing, and the load-displacement curve had no obvious yield point. In addition, the pullout load on the pile improved with the pad eye depth at the same pad eye displacement, and the pullout load significantly increased when the pad eye depth varied from $0.67L$ to $0.75L$. It can be indicated that the failure mode of the pile changed from vertically dominated pulling to vertical and horizontal translation with rotation as the pad eye position varied from $0.67L$ to $0.75L$.

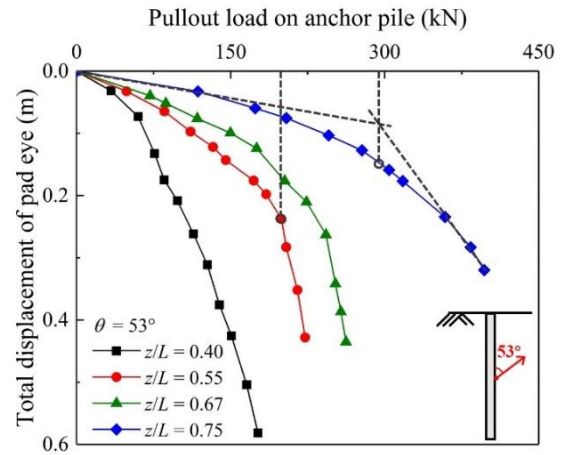


Figure 4. Load-displacement curves with different pad eye positions

3.2 Pullout bearing capacity

The pullout bearing capacity of the pile can be evaluated from the load-displacement curves. According to Bhardwaj and Singh (2014), for a curve with a stable stage, the pullout bearing capacity was obtained at the point on the curve where a large displacement derived for a small increment of load. For a curve without an obvious yield point, the pile capacity was taken as the load corresponding to the intersection of the two tangent lines drawn through the initial and final stage of the curve. Based on the methods, the pullout bearing capacity was determined, as shown in Table 1. With the increase of pad eye depth, the bearing capacity of anchor pile gradually increased. Compared with the pile loaded at $z = 0.40L$, the pile bearing capacity increased by 0.45 times, 0.76 times and 1.31 times in that with $z = 0.55L$, $0.67L$ and $0.75L$, respectively. Bang et al. (2011) conducted centrifuge model tests on suction anchors in sand, and

the effect laws of the pad eye position on the pullout capacity were in agreement with the results from this study. In the anchor pile design, the pad eye should be arranged at the lower part of the anchor pile, which can provide sufficient bearing capacity to resist environmental loads.

The pad eye position determined the pile rotation, affecting the bearing capacity of the anchor pile. In order to reveal the influencing mechanism of the pad eye position on the pile bearing capacity, the model pile profiles under the initial condition and peak load were compared, as shown in Figure 5. The figures represented the model with a pad eye position of $0.40L$, $0.55L$, $0.67L$ and $0.75L$ from left to right. The motion mode of anchor pile included horizontal and vertical translation with overall rotation, and lateral deflection of the pile occurred when $z/L = 0.67$ and 0.75 . When $z/L = 0.40$ and 0.55 , the anchor pile rotated towards the loading side (forward rotation). As the pad eye depth increased from $0.40L$ to $0.55L$, the rotation angle of the anchor pile decreased and the translation direction was closer to the horizontal. As a result, more passive earth pressure was mobilized by the anchor pile, which improved the pile bearing capacity. When $z/L = 0.67$ and 0.75 , the anchor pile rotated to the non-loading side (backward rotation), and the horizontal displacement at the pile bottom was large, which fully mobilized the passive earth pressure of deeper soil. When $z/L = 0.40$ and 0.55 , the horizontal displacement at the pile head was large, and the passive earth pressure of shallow soil was mobilized. Therefore, the bearing capacity of anchor pile is higher when $z/L = 0.67$ and 0.75 . As the pad eye depth increased from $0.67L$ to $0.75L$, the total rotation angle of the pile bottom caused by lateral deflection and overall rotation decreased, and the horizontal displacement of the pile bottom increased about 24%. Therefore, the passive earth pressure in deep soil could be more fully mobilized, improving the bearing capacity of the anchor pile. The pile rotation feature with the pad eye position was consistent with the findings of previous studies on suction anchor performances in clay (Guo et al., 2018; Xiong et al., 2024).

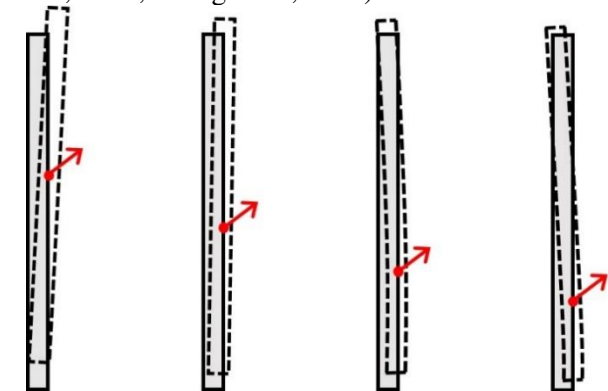


Figure 5. Pile motion modes with different pad eye positions

3.3 Soil displacement field

The speckle field images of the transparent sand sample were captured during the testing process. Afterwards, the two-dimensional soil displacement field on the loading side of the pile was calculated using PIVview2C software. The pile with pad eye positions of $0.67L$ and $0.75L$ under the maximum pullout load was taken as the example, and the soil displacement vector and contour are shown in Figure 6. The horizontal distance (x), the soil depth (z) and the soil displacement were normalized by the pile diameter.

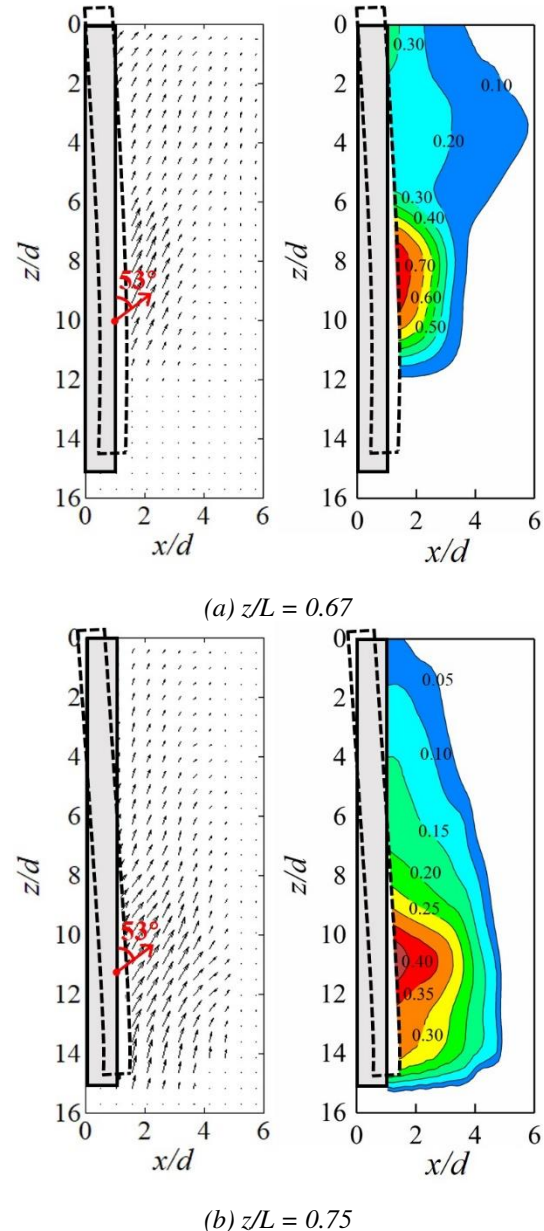


Figure 6. Normalized soil displacement vector and contour under different pad eye positions

Regardless of the pad eye positions, the soil moved away from the pile and upwards. The largest soil displacement was around the pad eye. The soil displacement was gradually decreased with the

increasing of the horizontal distance between the pile and the soil and the increasing distance between the pad eye and the soil in the depth direction. At $z/L = 0.67$, the obvious soil displacement was located at $0\sim 1.6d$ away from the pile side and $6.3\sim 10.7d$ below the soil surface. As the pad eye depth increased from $0.67L$ to $0.75L$, the value and zone of soil displacement decreased at $0\sim 6.5d$ below the soil surface. However, the soil influence range and displacement value (especially horizontal displacement) increased when the soil depth exceeded $10.8d$. The soil displacement increased by 0.30 times and the ratio of horizontal displacement to vertical displacement increased by 0.36 times. The effective stress and deformation modulus of deep soil were greater than that of shallow soil, which could provide greater soil resistance to the anchor pile. Therefore, the bearing capacity of anchor pile gradually increased with the pad eye depth.

4 CONCLUSIONS

In this paper, centrifugal model tests combined with transparent sand were performed to study the anchor pile response and soil displacement field under oblique pullout load, and the influence of pad eye position on the test results was analyzed. The main conclusions were summarized as follows:

Regardless of pad eye position, it was apparent that the load versus displacement behavior was nonlinear. The pile pushed the soil to move outwards and upwards, and the largest soil displacement was around the loading point. With the increasing pad eye depth, the rotation direction of the anchor pile gradually changed from forward rotation to backward rotation, and the influence range and displacement (especially horizontal displacement) of deep soil increased, leading to higher pullout bearing capacity. Compared with the bearing capacity of the pile with $z/L = 0.40$, the pile capacity increased by 0.45 times, 0.76 times and 1.31 times when $z/L = 0.55$, 0.67 and 0.75 , respectively. As the pad eye depth increased from $0.67L$ to $0.75L$, the failure mode of anchor piles changed from vertically dominated pulling to combined mode, the displacement value and ratio of horizontal to vertical displacement of deep soil increased by 0.30 times and 0.36 times, respectively.

This paper aims to offer initial introduction about the relationship between the soil displacement field and anchor pile response under different pad eye positions. The effects of installation methods, aspect ratios, pile flexibility and loading angles need to be further studied.

AUTHOR CONTRIBUTION STATEMENT

Zhongtao Wang: Conceptualization, Methodology, Supervision, Funding acquisition, Writing- Reviewing and Editing. **Guangyu Luo:** Conceptualization, Methodology, Data curation, Formal Analysis, Writing- Original draft, Investigation.

ACKNOWLEDGEMENTS

The authors gratefully acknowledge the financial support of the National Natural Science Foundation of China (Grant Nos. 41772296 and 52331010).

REFERENCES

- Aubeny, C.P., Han, S.W., Murff, J.D., (2003). Inclined load capacity of suction caissons. *International Journal for Numerical and Analytical Methods in Geomechanics*, 27: 1235-1254. 10.1002/nag.319
- Bang, S., Jones, K.D., Kim, K.O., Kim, Y.S., Cho, Y., (2011). Inclined loading capacity of suction piles in sand. *Ocean Engineering*, 38: 915-924. 10.1016/j.oceaneng.2010.10.019
- Bhardwaj, S., Singh, S.K., (2015). Pile capacity under oblique loads – evaluation from load–displacement curves. *International Journal of Geotechnical Engineering*, 9(4): 341-347. 10.1179/1939787914Y.0000000072
- Black, J.A., (2015). Centrifuge modelling with transparent soil and laser aided imaging. *Geotechnical Testing Journal*, 38(5): 631-644. 10.1520/GTJ20140231
- Cheng, L., Hossain, M.S., Hu, Y., Kim, Y.H., Ullah, S.N., (2021). Failure envelope of suction caisson anchors subjected to combined loadings in sand. *Applied Ocean Research*, 114: 102801. 10.1016/j.apor.2021.102801
- Dyson, G.J., Randolph, M.F., (2001). Monotonic lateral loading of piles in calcareous sand. *Journal of Geotechnical and Geoenvironmental Engineering*, 127(4): 346-352. 10.1061/(ASCE)1090-0241(2001)127:4(346)
- Ezzein, F.M., Bathurst, R.J., (2011). A transparent sand for geotechnical laboratory modeling. *Geotechnical Testing Journal*, 34(6): 590-601.
- Gao, Y., Qiu, Y., Li, B., Li, D., Sha, C., Zheng, X., (2013). Experimental studies on the anti-uplift behavior of the suction caissons in sand. *Applied Ocean Research*, 43: 37-45. 10.1016/j.apor.2013.08.001
- Georgiadis, M., Anagnostopoulos, C., Saflekou, S., (1992). Centrifugal testing of laterally loaded piles

- in sand. *Canadian Geotechnical Journal*, 29: 208-216. 10.1139/t92-024
- Guo, Z., Jeng, D., Guo, W., Wang, L., (2018). Failure mode and capacity of suction caisson under inclined short-term static and one-way cyclic loadings. *Marine Georesources & Geotechnology*, 36(1): 52-63. 10.1080/1064119x.2017.1279244
- Guzman, I.L., Iskander, M., Suescun-Florez, E., Omidvar, M., (2014). A transparent aqueous-saturated sand surrogate for use in physical modeling. *Acta Geotechnica*, 9: 187-206. 10.1007/s11440-013-0247-2
- Huang, T., O'loughlin, C., Gaudin, C., Tian, Y., Lu, T., (2020). Drained response of rigid piles in sand under an inclined tensile load. *Géotechnique Letters*, 10(1): 30-37. 10.1680/jgele.19.00028
- Kong, G., Cao, Z., Zhou, H., Sun, X., (2015). Analysis of piles under oblique pullout load using transparent-soil models. *Geotechnical Testing Journal*, 38(5): 725-738. 10.1520/GTJ20140109
- Ramadan, M.I., Butt, S.D., Popescu, R., (2013). Offshore anchor piles under mooring forces: centrifuge modeling. *Canadian Geotechnical Journal*, 50(4): 373-381. 10.1139/cgj-2012-0250
- Santiago, P.C., Saboya, F., Tibana, S., Reis, R.M., Borges, R.G., (2020). Centrifuge modelling of a combined pile-type anchor subjected to general inclined loading. *Marine Structures*, 74(1): 102815. 10.1016/j.marstruc.2020.102815
- Song, Z., Hu, Y., O'Loughlin C., Randolph, M.F., (2009). Loss in anchor embedment during plate anchor keying in clay. *Journal of Geotechnical and Geoenvironmental Engineering*, 135(10): 1475-1485. 10.1061/(ASCE)GT.1943-5606.0000098
- Xiong, G., Fu, D., Zhu, B., Lai, Y., (2024). Centrifuge modelling of suction anchor subjected to inclined load in soft clay. *Rock and Soil Mechanics*, 45(5): 1472-1480. 10.16285/j.rsm.2023.0869
- Zhao, L., Gaudin, C., O'Loughlin, C.D., Hambleton, J.P., Cassidy, M.J., Herduin, M., (2019). Drained capacity of a suction caisson in sand under inclined loading. *Journal of Geotechnical and Geoenvironmental Engineering*, 145(2): 04018107. 10.1061/(ASCE)GT.1943-5606.0001996

INTERNATIONAL SOCIETY FOR SOIL MECHANICS AND GEOTECHNICAL ENGINEERING



This paper was downloaded from the Online Library of the International Society for Soil Mechanics and Geotechnical Engineering (ISSMGE). The library is available here:

<https://www.issmge.org/publications/online-library>

This is an open-access database that archives thousands of papers published under the Auspices of the ISSMGE and maintained by the Innovation and Development Committee of ISSMGE.

The paper was published in the proceedings of the 5th International Symposium on Frontiers in Offshore Geotechnics (ISFOG2025) and was edited by Christelle Abadie, Zheng Li, Matthieu Blanc and Luc Thorel. The conference was held from June 9th to June 13th 2025 in Nantes, France.